

(Al)GaInP/GaAs Tandem Solar Cells For Power Conversion at Elevated Temperature and High Concentration

Emmett E. Perl¹, John Simon¹, Daniel J. Friedman¹, Nikhil Jain¹, Paul Sharps², Claiborne McPheeters², Yukun Sun³, Minjoo L. Lee³, Myles A. Steiner¹

¹National Renewable Energy Laboratory, Golden, Colorado, United States

²SolAero Technologies Corp., Albuquerque, New Mexico, United States

³University of Illinois at Urbana-Champaign, Urbana, Illinois, United States

Abstract — We demonstrate dual-junction (Al)GaInP/GaAs solar cells designed for operation at 400°C and 1000x concentration. For the top junction, we compare (Al)GaInP solar cells with room-temperature bandgaps ranging from 1.9-2.0eV. At 400°C, we find that ~1.9eV GaInP solar cells have a higher open-circuit voltage and a lower sheet resistance than higher bandgap (Al)GaInP solar cells, giving them a clear advantage in a tandem configuration. Dual-junction GaInP/GaAs solar cells are fabricated, and we show temperature-dependent external quantum efficiency, illuminated current-voltage, and concentrator measurements from 25-400°C. We measure a power conversion efficiency of $16.4 \pm 1\%$ at 400°C and 345 suns for the best dual-junction cell, and discuss multiple pathways to improving the performance further. After undergoing a 200 hour soak at 400°C, the dual-junction device shows a relative loss in efficiency of only ~1%.

Index Terms — III-V and concentrator photovoltaics (PV), PV cells, semiconductor materials, solar energy, high temperature.

I. INTRODUCTION

It is well established that the efficiency of a typical solar cell decreases as the temperature rises, and most solar cell systems are therefore designed to operate as close to room temperature as possible [1-8]. Some applications, however, may *require* high temperature operation. For example, a number of hybrid photovoltaic-thermal (PV-T) systems and near-sun space missions have called for the development of reliable solar cells that can operate efficiently at temperatures as high as 400°C [9-13]. It is critical, however, to first develop a prototype cell before any system could viably consider the use of a high-temperature solar array.

We reported preliminary work on the development of high-temperature tandem solar cells in [14]. That paper included details on our temperature-dependent cell efficiency model, and we determined that a dual-junction design with a 1.9-2.0eV (Al)GaInP top junction and 1.4eV GaAs bottom junction is nearly optimal for operation at 400°C. That paper also contained studies comparing the stability of various front metallizations and antireflection coating (ARC) designs at high-temperature.

In this enhanced paper, we include a number of significant new results. First, we include a detailed description of the measurement challenges inherent to characterizing dual-junction solar cells at high temperatures. Second, we compare the high temperature performance of (Al)GaInP top cells with varying aluminum composition and bandgap (E_g) for use as the

top junction in an (Al)GaInP/GaAs tandem. Third, we demonstrate an improved dual-junction design with a peak efficiency of 16.4% at 400°C and 345x concentration. Finally, we soak the dual-junction cell for 200 hours at 400°C and measure a relative efficiency drop of only ~1%.

II. EXPERIMENTAL METHODS

All solar cells were grown upright using a custom-built atmospheric pressure organometallic vapor-phase epitaxy (OMVPE) vertical reactor on zinc-doped (001) GaAs substrates, miscut 6° toward the <111>A direction. The GaAs subcell was grown at 650°C and is composed of a 300 nm zinc-doped GaInP back surface field (BSF), a 3 μm zinc-doped GaAs base, a 100 nm selenium-doped GaAs emitter, and a 25 nm selenium-doped GaInP window layer. We explored many different structures and growth conditions for the (Al)GaInP top subcell; additional details can be found elsewhere [15,16]. The two subcells were connected in series with a tunnel junction composed of 50 nm of carbon-doped AlGaAs, 12 nm of silicon-doped GaAs, and 50 nm of selenium-doped AlGaAs. Gold back contacts were electroplated onto the backside of the GaAs substrate and front contacts consisting of Ti/Pt/Al/Pt (50/50/3000/50 nm) were deposited using electron-beam evaporation. Standard cleanroom photolithography and wet chemical etching techniques were used for mesa isolation, and a bi-layer ARC composed of TiO₂/Al₂O₃ was deposited onto the front of the dual-junction solar cells. Additional studies on the stability of the front metallization and ARC at high-temperature are reported in [14].

During cell measurements, the sample temperature was controlled using a Linkam Instruments HFS600E-PB4 temperature controlled stage capable of heating up to 600°C. Details on the techniques for taking high-temperature external quantum efficiency (EQE), one-sun illuminated current-voltage (LIV), and high-concentration LIV measurements of single-junction cells were discussed previously [8].

While measuring the EQE of single-junction (Al)GaInP and GaAs cells over the entire temperature range was straightforward, the dual junction cells presented some challenges. We were unable to measure the EQE of the GaAs subcell in a tandem configuration above 300°C. At the highest temperatures, there is a non-zero slope in the GaAs subcell JV curve at short-circuit (J_{sc}) and in reverse bias, which results

from the increasing dark currents at elevated temperatures as is shown in reference [8]. This makes it difficult to properly adjust the light and voltage bias to isolate the GaAs subcell in a tandem configuration without overloading the measurement electronics. To estimate the EQE of the GaAs subcell above 300°C, we grew a filtered GaAs single-junction cell similar to the bottom junction of the two-junction cell. Since this cell does not require any light or voltage bias, we are able to reliably measure the EQE.

LIV measurements were taken using a custom-built solar simulator that uses a broadband xenon lamp and adjustable high-brightness LEDs to properly calibrate the spectrum for a multi-junction solar cell. The stage height was adjusted such that the lamp spectrum, LED spectrum, reference cells, and solar cells were all measured in the same reference plane. To account for reflection off the quartz window and back surface of the Linkam stage, we determined separate attenuation factors for the LEDs and xenon lamp by comparing the J_{sc} of a single-junction device measured with and without the quartz window. Due to the geometry of the solar simulator and Linkam stage, these attenuation factors are different for each light source.

The one-sun light intensity was adjusted using the measured spectrum of the xenon lamp and LEDs, photocurrents from calibrated reference cells, attenuation factors from the light sources as described above, and the temperature-dependent EQE curves of the dual-junction and filtered GaAs single-junction cells. The procedure to compute spectral mismatch factors and determine the equivalent one-sun light intensity is described in [17,18]. Between 25°C and 300°C, we were able to reliably measure the EQE of the GaAs subcell in the dual-junction configuration, and the suns value computed using the spectral mismatch correction factor of the GaAs subcell differed by only 0.6% on average compared to the suns value computed using the spectral mismatch correction factor of the filtered GaAs single-junction. Above 300°C, we used the EQE of the GaAs single-junction to adjust the one-sun light intensity for the bottom junction; the error introduced by using the isotope QE is minimal.

Concentrator measurements were taken using a high-intensity pulsed solar simulator (HIPSS). This system has two low-pressure xenon arc lamps that deliver millisecond-long pulses of light to the cell, enough time to take an IV measurement. The concentration is determined from the ratio of the measured J_{sc} to the one-sun J_{sc} , assuming linearity of the photocurrent. We did not adjust the spectrum of the HIPSS, and this could lead to a small increase in the fill factor (FF) due to current-mismatch and slight overestimation of the cell efficiency under concentration [19]. There are also a few external series resistances, between the back of the cell and the voltage probe, that cannot be removed when taking a four-probe measurement, and these would lead to a small underestimation in the cell FF and efficiency under concentration.

III. DETERMINATION OF THE TOP JUNCTION MATERIAL

We studied (Al)GaInP solar cells with room-temperature bandgaps between ~1.9eV (0% Al) and ~2.0eV (~12% Al) for use as the top junction in a tandem cell optimized for operation at 400°C. Previously, we reported details on AlGaInP solar cells at one-sun and 25°C, and demonstrated a bandgap-voltage offset (W_{oc}) of 500mV or less for cells with bandgaps between 1.9-2.1eV [15]. Because of these low W_{oc} values, we consistently measured a higher open-circuit voltage (V_{oc}) for higher bandgap (Al)GaInP cells at room temperature, as one would expect for well-behaved cells.

A plot of the V_{oc} as a function of temperature, extracted from HIPSS measurements at a J_{sc} of 10A/cm² (~1000 suns), is shown in Fig. 1 for (Al)GaInP solar cells with aluminum compositions ranging from 0%-12%. Contrary to expectation, and in contrast to the room-temperature behavior just

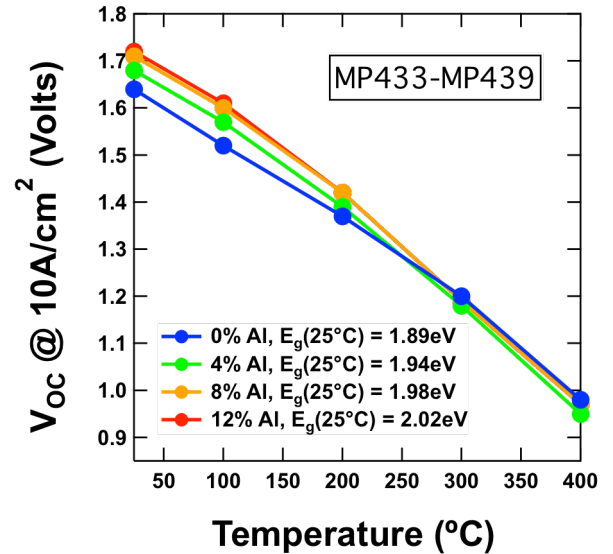


Figure 1 Temperature-dependent V_{oc} of (Al)GaInP solar cells of varying aluminum composition, extracted from HIPSS measurements at a photocurrent density of 10A/cm².

discussed, we observe that the V_{oc} of our GaInP solar cells overtakes the V_{oc} of the higher bandgap (Al)GaInP cells as the temperature is increased above 300°C. At 400°C, there is no longer any voltage advantage associated with increasing the top cell bandgap. One important reason we observe this is related to the temperature-dependence of the J_{01} dark saturation current densities, which we discuss in detail elsewhere [8]. The dominant temperature dependence for J_{01} has an E term in the exponent, which will cause the dark currents of high bandgap solar cells to rise more rapidly with temperature than the dark currents of lower bandgap solar cells. This will cause the V_{oc} of higher bandgap solar cells to drop more rapidly as the temperature is increased. Additionally, we observe a larger bandgap-voltage offset ($W_{oc} = E/q - V_{oc}$) for (Al)GaInP solar cells with a higher bandgap and aluminum composition [15].

This will also erode the voltage advantage associated with increasing the top cell bandgap.

Current matching is another important consideration when optimizing a dual-junction solar cell for maximum efficiency as a function of temperature [6]. In [8], we reported temperature-dependent LIV measurements of $\text{Al}_{0.12}\text{Ga}_{0.39}\text{In}_{0.49}\text{P}$ and filtered GaAs single-junction cells, and measure a $\sim 1.5x$ higher J_{sc} for the filtered GaAs bottom junction at 400°C . This severe current mismatch will limit the achievable efficiency for an $\text{Al}_{0.12}\text{Ga}_{0.39}\text{In}_{0.49}\text{P}/\text{GaAs}$ tandem. On the other hand, we found that an optically thick GaInP/GaAs tandem is slightly bottom limited at 400°C . In this configuration, current matching can be achieved by thinning the GaInP top cell.

We also considered the effects of aluminum composition on the series resistance. The sheet resistance (R_{sheet}) of the emitter can make up a large fraction of the total series resistance of a solar cell, and this can significantly reduce the FF and photocurrent (because of shadowing from the grid fingers required to mitigate the resistance), and hence the efficiency at high concentration.

Fig. 2 shows R_{sheet} , measured using the standard transfer length method (TLM), versus temperature for GaInP and $\text{Al}_{0.12}\text{Ga}_{0.39}\text{In}_{0.49}\text{P}$ solar cells. As the temperature is raised to 400°C , there is a $\sim 2.5x$ increase in R_{sheet} for the $\text{Al}_{0.12}\text{Ga}_{0.39}\text{In}_{0.49}\text{P}$ cell and $\sim 1.9x$ increase in R_{sheet} for the GaInP cell, and this will increase the relative contribution of R_{sheet} to the overall series resistance at elevated temperatures. The advantage of the GaInP over the $\text{Al}_{0.12}\text{Ga}_{0.39}\text{In}_{0.49}\text{P}$ appears to compound as the

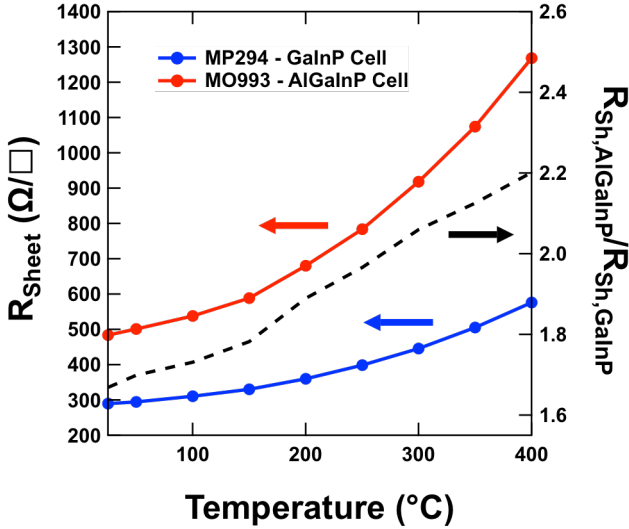


Figure 2 Temperature-dependent sheet resistance of GaInP (blue) & AlGaInP (red) solar cells measured from TLM. The black dashed line shows the ratio of the sheet resistance for each cell, and indicates that the sheet resistance is increasing more rapidly for the AlGaInP cell than for the GaInP cell.

temperature is increased, as is evident from the black dashed line comparing the ratio of R_{sheet} for the GaInP and AlGaInP solar cells. We expect that the $\sim 2.2x$ lower R_{sheet} at 400°C will help a GaInP/GaAs tandem attain a higher FF and efficiency at concentration compared to a dual-junction cell with a higher bandgap (Al)GaInP top junction.

Fig. 3 shows the specific contact resistivity (ρ_c) of the GaInP cell as a function of operating temperature, also measured by TLM. We observe a $\sim 5x$ reduction in ρ_c as the temperature is increased from 25°C to 400°C . One possible explanation is that raising the temperature will increase thermionic emission over any resistive barrier between the emitter and the metal contacting layer, thereby reducing ρ_c . This trend suggests that the relative contribution of ρ_c to the overall series resistance will decrease at elevated temperatures. We also measure a $\sim 2x$ increase in the grid resistance (not shown) as the temperature is increased from 25°C to 400°C , which is consistent with the temperature coefficients reported for the resistivity of aluminum [20].

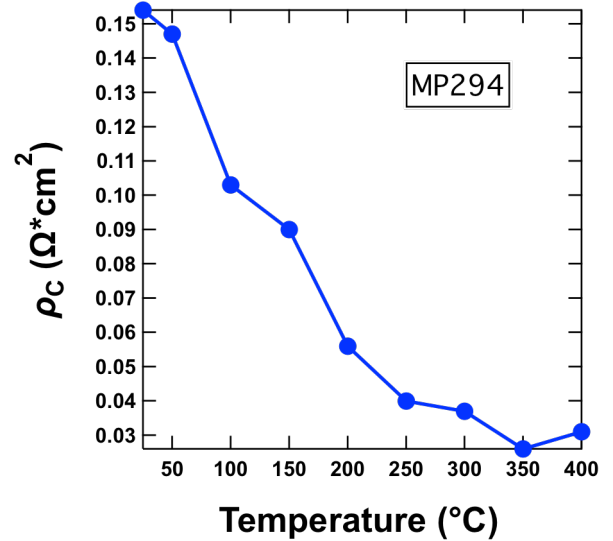


Figure 3 Temperature-dependent specific contact resistivity (ρ_c) for a GaInP solar cell.

Based on voltage, current, and series resistance considerations of the best top cells presently available, it is clear that the GaInP top cell is the better choice for the high-temperature tandem.

IV. TANDEM CELL RESULTS AND DISCUSSION

We have grown (Al)GaInP/GaAs tandem solar cells with varying aluminum content, but always found that GaInP/GaAs tandems had a higher efficiency at 400°C for the reasons discussed in the previous section. In this section, we will show results for the best GaInP/GaAs tandem measured to date.

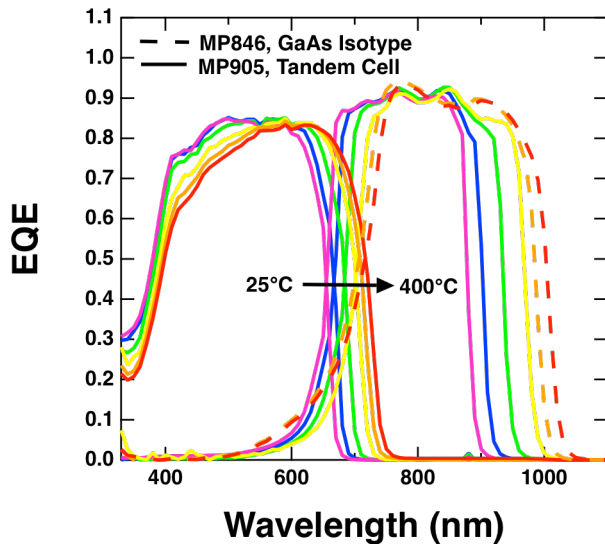


Figure 4 EQE for a GaInP/GaAs solar cell measured from 25-400°C. The EQE of the bottom GaAs cell could not be measured above 300°C due to the high saturation dark current. The dashed lines show the EQE of a filtered GaAs single-junction at these elevated temperatures.

Fig. 4 shows the temperature dependent EQE of the GaInP/GaAs cell. As discussed earlier, the EQE of the GaAs bottom junction could not be measured above 300°C due to the non-zero slope in the GaAs LIV curve. The dashed lines show the EQE of a filtered GaAs single-junction measured at

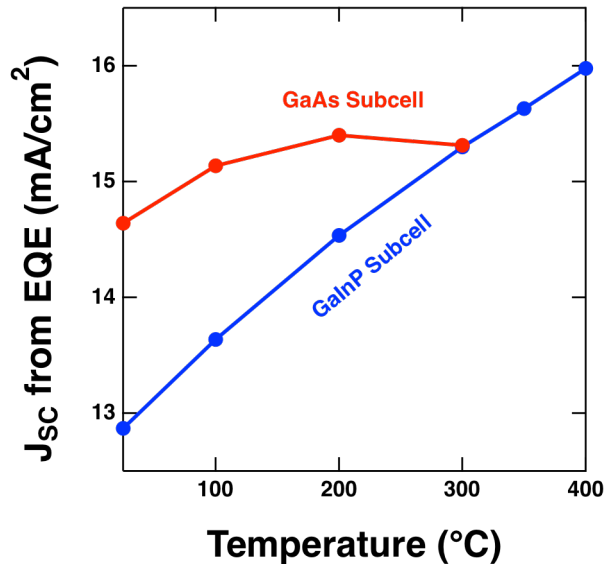


Figure 5 J_{sc} calculated from the EQE curves for the GaInP subcell (blue) and the GaAs subcell (red).

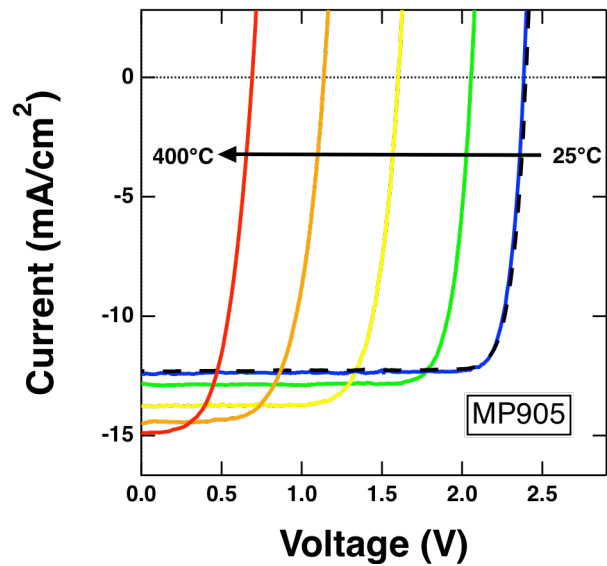


Figure 6 Temperature-dependent LIV measurements for the GaInP/GaAs tandem taken at a light intensity of one sun under the AM1.5D spectrum. The black dashed curve shows the LIV curve of the same device taken without the Linkam stage at 25°C.

350°C and 400°C, and these act as a good approximation for the EQE of the bottom subcell at the highest temperatures. The data clearly show the redshift in all of the curves as the operating temperature is increased. This redshift is a result of the decreasing bandgap of all of the epitaxial-grown materials at elevated temperatures. The short-wavelength EQE of the GaInP cell also appears to decrease at elevated temperatures. On other GaInP/GaAs tandem cells, we measured the 25-400°C EQE before and after the ARC deposition. Prior to the ARC deposition, we did not observe any significant decrease of EQE at short wavelengths when the temperature was increased. On the other hand, we consistently observed this short-wavelength EQE drop at elevated temperatures for cells with a TiO₂/Al₂O₃ ARC. This suggests that the reduced EQE at low wavelengths is caused by increased absorption in the TiO₂/Al₂O₃ ARC at elevated temperatures.

Fig. 5 shows estimated photocurrents of the two subcells computed by integrating the product of the EQE and AM1.5D spectrum. While the GaInP subcell is current-limiting at room temperature, its photocurrent increases more rapidly than the photocurrent of the GaAs subcell and at 300°C, the tandem device is very nearly current matched. While we don't have EQE measurements of the GaAs subcell at 400°C, trends in the EQE and LIV curves for our filtered GaAs single-junction cell indicate that the tandem remains nearly current matched at 400°C.

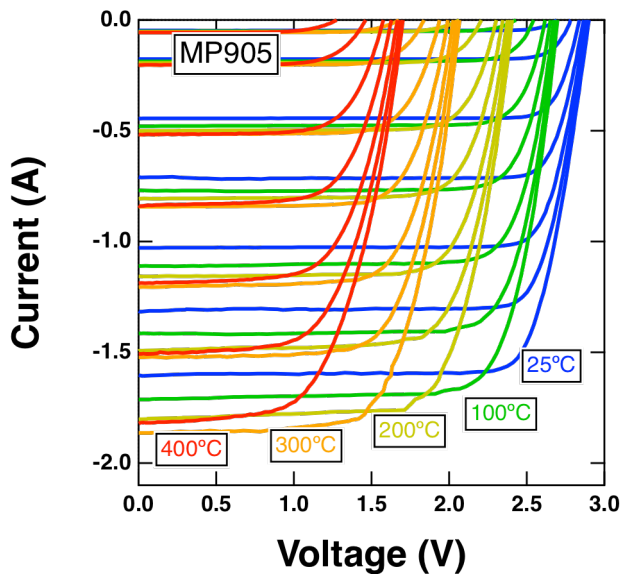


Figure 7 Temperature-dependent concentrator measurements for the GaInP/GaAs tandem taken using the HIPSS.

Fig. 6 shows one-sun LIV measurements of the GaInP/GaAs tandem from 25-400°C. As expected, there is a significant reduction in the V_{oc} as the temperature is increased resulting from the exponential increase in the J_0 and J_{sc} dark currents. There is also a small increase in the J_{sc} resulting from the bandgap reduction at elevated temperatures. This bandgap shift, illustrated in Fig. 4, will improve current matching and increase the absorption range of the dual-junction device, thereby increasing the J_{sc} . The increasing J_{sc} is consistent with the trends shown in Fig. 5. The black dashed line shows the

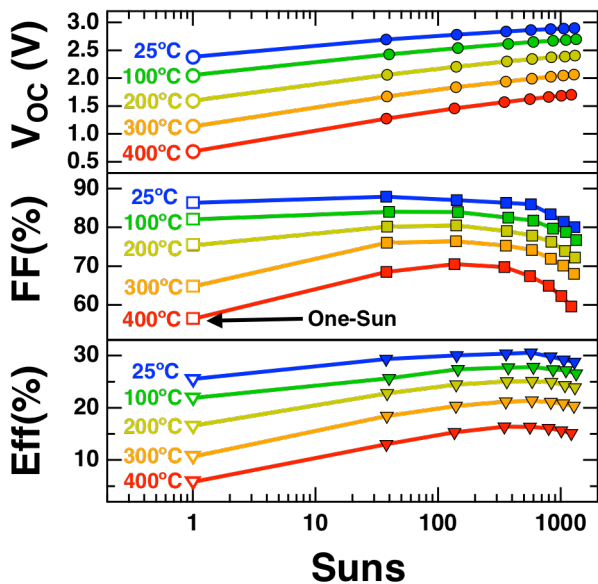


Figure 8 V_{oc} , FF, and efficiency as a function of concentration and temperature for the GaInP/GaAs dual-junction solar cell. IV data taken at one-sun (open markers) were taken on a custom-built solar simulator and are shown in Fig. 6. IV data at concentration (solid markers) were taken on a HIPSS and are shown in Fig. 7.

one-sun LIV curve of the tandem device measured at room temperature without the Linkam stage, and the very close agreement to the blue curve gives credence to our procedure for calibrating the one-sun light intensity for dual-junction cells in the Linkam stage.

Fig. 7 shows concentrator measurements for the GaInP/GaAs tandem solar cell from 25-400°C, with the concentration ranging from ~30-1500 suns. The cells are stable and the data are reproducible at temperatures up to 400°C, and the tunnel junction is clearly able to handle the high photocurrents at all temperatures. The drop in V_{oc} with temperature, which dominates the efficiency loss, is also apparent.

From these curves, we are able to extract the V_{oc} , FF, and efficiency as a function of both temperature and concentration. These plots are shown in Fig. 8. At 400°C, the efficiency peaks at $16.4 \pm 1\%$ at a concentration of 345 suns and remains above 15% at 1000 suns. We also measure a peak efficiency of $21.4 \pm 1\%$ at 300°C, $25.1 \pm 2\%$ at 200°C, $27.8 \pm 2\%$ at 100°C, and $30.6 \pm 2\%$ at 25°C; further optimization could improve the cell efficiency at these operating temperatures.

There are multiple pathways to increasing the 400°C efficiency further. A reduced series resistance would help improve the FF at high concentrations, and this could significantly reduce the efficiency rollover above ~300 suns. A circuit model with two series-connected $n=1$ diodes, adjusted to match the empirical V_{oc} and one-sun J_{sc} of our device yields an efficiency of ~19% at 400°C and 1000x concentration when there is no series resistance. Reducing the series resistance could also lead to a higher one-sun J_{sc} since shadowing of the grid fingers, required to mitigate the resistance, could be reduced. Improvements to the grid design and ARC could also help to improve the J_{sc} and efficiency at

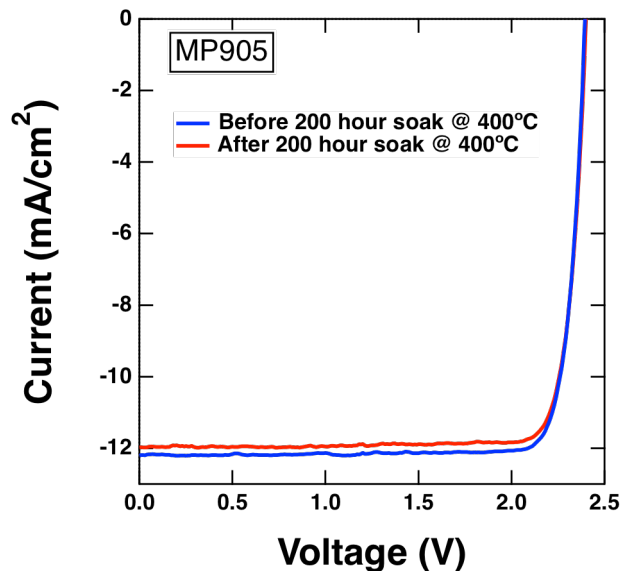


Figure 9 One-sun LIV curves for the GaInP/GaAs tandem taken at room temperature before and after soaking at 400°C for 200 hours.

400°C. The EQE shown in Fig. 4 peaks at ~80% for the GaInP cell and ~90% for the GaAs cell, values that are 5-10% lower than some of the best GaInP and GaAs cells reported in the literature [21-24]. We expect that the J_{sc} could be marginally improved by further optimizing the absorber layer thicknesses, modifying the ARC design to reduce absorption at high temperatures, and developing narrow high-aspect grid fingers with optimized finger spacing. We also measure a V_{oc} that is ~100mV lower than expected from a drift-diffusion model of a solar cell that assumes that only the intrinsic carrier concentration (n_i) is temperature dependent. A detailed study exploring this deviation will be reported elsewhere [25]. Despite these challenges, our analysis indicates that there is no fundamental barrier to improving the efficiency of a dual-junction solar cell to >20% at 400°C and 1000x concentration.

Finally, Fig. 9 shows LIV measurements, taken at one-sun and 25°C, for the GaInP/GaAs tandem before and after a 200 hour soak at 400°C in a tube furnace with flowing nitrogen. During this time, the cells were electrically isolated and the intensity of ambient light was uncontrolled. After the high-temperature soak, we observe no V_{oc} drop and only a small ~1% drop in the cell efficiency. While more detailed studies exploring the activation energy of different degradation mechanisms are on-going, these preliminary results suggest that these cells are capable of surviving at 400°C for long periods of time with minimal degradation.

V. SUMMARY

In summary, we demonstrate dual-junction (Al)GaInP/GaAs solar cells designed for operation at elevated temperature and high concentration. (Al)GaInP solar cells with room temperature bandgaps ranging from 1.9-2.0eV are compared for use as the top junction in an (Al)GaInP/GaAs tandem. Relative to higher bandgap (Al)GaInP designs, we found that GaInP solar cells exhibited a higher V_{OC} , lower R_{Sheets} , and improved current matching to a GaAs bottom junction at 400°C. GaInP/GaAs tandems were fabricated with a durable bi-layer ARC, a robust tunnel junction, and a stable high-temperature metallization, and temperature-dependent EQE, LIV, and concentrator measurements were taken from 25-400°C. A peak efficiency of $16.4 \pm 1\%$ was measured for the GaInP/GaAs tandem at 400°C and 345x concentration, with the efficiency still $>15 \pm 1\%$ at 1000x. After undergoing a 200 hour soak at 400°C, we measure a relative loss in efficiency of only ~1% for the dual-junction device.

ACKNOWLEDGEMENTS

The authors are pleased to thank W. Olavarria, M. Young and C. Beall at NREL for processing work, and John Geisz for useful conversations. This work was supported by the U.S. Department of Energy through the ARPA-E FOCUS program under Award DE-AR0000508, and through contract DE-AC36-08GO28308 with the National Renewable Energy

Laboratory. The U.S. Government retains, and the publisher by accepting the article for publication acknowledges that the U.S. Government retains, a nonexclusive, paid up, irrevocable, worldwide license to publish or reproduce the published form of this work, or allow others to do so, for U.S. Government purposes.

REFERENCES

- [1] C. Algora, *Handbook on concentrator photovoltaic technology*: John Wiley & Sons, 2016.
- [2] A. L. Fahrenbruch, *et al.*, *Fundamentals of Solar Cells Photovoltaic Solar Energy Conversion*. New York: Academic Press, 1983.
- [3] J. C. Fan, "Theoretical temperature dependence of solar cell parameters," *Solar Cells*, vol. 17, pp. 309-315, 1986.
- [4] D. J. Friedman, "Modelling of tandem cell temperature coefficients," in *25th IEEE Photovoltaic Specialists Conference*, Washington D.C., 1996, pp. 89-92.
- [5] D. J. Friedman, *et al.*, "High-efficiency III-V multijunction solar cells," in *Handbook of Photovoltaic Science and Engineering, 2nd Ed.*, A. Luque and S. Hegedus, Eds., ed Chichester UK: Wiley, 2011, pp. 314-364.
- [6] D. J. Friedman, *et al.*, "Spectral and concentration sensitivity of multijunction solar cells at high temperature," in *44th IEEE Photovoltaic Specialists Conference*, Washington D.C., 2017.
- [7] H. J. Hovel, *Solar Cells* vol. 11. New York: Academic Press, 1975.
- [8] E. E. Perl, *et al.*, "Measurements and modeling of III-V solar cells at high temperatures up to 400°C," *IEEE Journal of Photovoltaics*, vol. 6, pp. 1345-1352, 2016.
- [9] T. T. Chow, "A review on photovoltaic/thermal hybrid solar technology," *Applied energy*, vol. 87, pp. 365-379, 2010.
- [10] Y. Vorobiev, *et al.*, "Thermal-photovoltaic solar hybrid system for efficient solar energy conversion," *Solar energy*, vol. 80, pp. 170-176, 2006.
- [11] H. M. Branz, *et al.*, "Hybrid solar converters for maximum exergy and inexpensive dispatchable electricity," *Energy Environ. Sci.*, vol. 8, p. 3083, 2015.
- [12] G. A. Landis, *et al.*, "High-temperature solar cell development," in *18th Space Photovoltaic Research and Technology Conference*, 2005, pp. 241-247.
- [13] O. V. Sulima, *et al.*, "High-temperature AlGaP/GaP solar cells for NASA space missions," in *Photovoltaic Energy Conversion, 2003. Proceedings of 3rd World Conference on*, 2003, pp. 737-740.
- [14] M. A. Steiner, *et al.*, "AlGaInP/GaAs tandem solar cells for power conversion at 400°C and 1000X concentration," in *44th IEEE Photovoltaic Specialists Conference*, Washington D.C., 2017.

- [15] E. E. Perl, *et al.*, "Development of high-bandgap AlGaInP solar cells grown by organometallic vapor-phase epitaxy," *IEEE Journal of Photovoltaics*, vol. 6, pp. 770-776, 2016.
- [16] E. E. Perl, *et al.*, "Development of a 2.0 eV AlGaInP solar cell grown by OMVPE," in *42nd IEEE Photovoltaic Specialists Conference*, New Orleans, LA, 2015, pp. 1-6.
- [17] K. Emery, "Performance and Efficiency Measurements of PV Devices," in *Advances in Solar Energy*. vol. 7, K. W. Boer, Ed., ed Boulder, CO: American Solar Energy Society, Inc., 1992, pp. 73-120.
- [18] K. Emery, "Measurement and Characterization of Solar Cells and Modules," in *Handbook of Photovoltaic Science and Engineering*, A. Luque and S. Hegedus, Eds., ed West Sussex, England: Wiley, 2003, p. 720.
- [19] C. R. Osterwald, *et al.*, "Concentrator cell efficiency measurement errors caused by unfiltered xenon flash solar simulators," in *AIP Conference Proceedings*, 2014, pp. 149-153.
- [20] R. O. Simmons, *et al.*, "Measurements of the high-temperature electrical resistance of aluminum: Resistivity of lattice vacancies," *Physical Review*, vol. 117, p. 62, 1960.
- [21] J. F. Geisz, *et al.*, "Enhanced external radiative efficiency for 20.8% efficient single-junction GaInP solar cells," *Appl. Phys. Lett.*, vol. 103, p. 041118, 2013.
- [22] P. T. Chiu, *et al.*, "Direct semiconductor bonded 5J cell for space and terrestrial applications," *IEEE J. Photovolt.*, vol. 4, pp. 493-497, 2014.
- [23] F. Dimroth, *et al.*, "Four-junction wafer-bonded concentrator solar cells," *IEEE Journal of Photovoltaics*, vol. 6, pp. 343-349, 2016.
- [24] R. M. France, *et al.*, "Quadruple-junction inverted metamorphic concentrator devices," *IEEE Journal of Photovoltaics*, vol. 5, pp. 432-437, 2015.
- [25] E. E. Perl, *et al.*, "Identification of the limiting factors for high-temperature GaAs, GaInP, and AlGaInP solar cells from device and carrier lifetime analysis," *Submitted*, 2017.